DOI: 10.1002/ejoc.200901423

Synthesis and Optical Properties of Cyanine Dyes as Fluorescent DNA Base Substitutions for Live Cell Imaging

Carolin Holzhauser,[a] Sina Berndl,[a] Florian Menacher,[a] Miriam Breunig,[b] Achim Göpferich,[b] and Hans-Achim Wagenknecht*[a]

Keywords: Thiazole orange / Nucleic acids / Oligonucleotides / Fluorescence / Energy transfer / Dyes/pigments

The chromophore of thiazole orange (**TO**) and its derivative **TO3** were incorporated synthetically as base surrogates into oligonucleotides using automated phosphoramidite chemistry. In comparison to **TO**, the **TO3** chromophore contains an extended carbomethine bridge that shifts the absorption and emission significantly to the red. (*S*)-1-Aminopropane-2,3-diol served as an acyclic linker between the phosphodiesters. This linker was attached either to the quinoline or the thiazole nitrogen of the **TO** and **TO3** dyes. The optical properties of **TO** and **TO3** were studied in different DNA base environments and with different opposite bases. Both dyes as fluorescent DNA base substitutions show a brightness that is sufficient for bioanalytic and imaging applications. Additionally the **TO3** dyes were combined as interstrand dimers, but in contrast to **TO** dimers, a red-shifted fluorescence was not observed. However, **TO** and **TO3** can be combined to an interstrand chromophore pair and a DNA hybridization-dependent energy transfer process can be obtained between the modifications. As a result, the emission is shifted from the **TO**-typical value of 530 nm to 670 nm. This concept can be applied for fluorescence imaging to monitor DNA delivery as well as processing inside living cells by confocal microscopy. In contrast to the non-covalently binding **TO** dyes, the **TO**- and **TO3**-modified oligonucleotides are cell-permeable.

Introduction

Bioanalysis and imaging of nucleic acids in chemical cell biology require bright and tailor-made fluorophores that can be linked covalently to DNA (or RNA). A variety of fluorescent dyes has been synthetically attached to oligonucleotides in order to detect the complementary sequential information and single base variations by enhanced emission intensity or quenching.[1–5] Especially molecular beacons have become powerful tools in a variety of DNA/RNA based applications.[6–9] However, simple changes of the fluorescence intensity at a given wavelength carry the risk of side effects causing artifacts in the fluorescence readout. Undesired emission quenching is a significant problem especially in cell imaging leading to false positive signals or reducing the sensitivity (S/B ratio). Hence, dual fluorescent oligonucleotide probes for imaging nucleic acids are needed which are bright as a single label and have the potential to change their emission maximum (= color) in the presence of the target. This has been realized e.g. as wavelength-shifting molecular beacons based on fluorescence resonance energy transfer processes (FRET).[10] However, the design of dual-labeled oligonucleotide probes which carry an energy donor (first label) that can be excited selectively beyond the UV (>450 nm) in combination with an energy acceptor (second label) that emits bright fluorescence in the visible spectrum due to a high FRET efficiency remains a challenge.

Currently, the excimer-induced red-shifting of the emission wavelength undergoes a renaissance with respect to DNA analytics. DNA with intrastrand and interstrand dimers mainly of pyrene and perylene exhibit strong excimer fluorescence[11–15] and can also be applied in molecular beacons.[16–19] However, the excitation of pyrene requires high-energy UV light, a circumstance that limits the bioanalytic and imaging applications significantly. Recently, we reported that the excitation of perylene bisimide pairs at 505 nm yields an excimer-type shift of the fluorescence by ca. 100 nm in DNA, and we applied it to quantify single base mismatches.[20] One of the major disadvantages of perylene bisimide in DNA, however, is the low quantum yield in certain DNA sequences due to fluorescence quenching by charge transfer processes especially with guanines.[21,22] In this context, thiazole orange (**TO**) represents a promising alternative. Among the brightly emitting and broadly applied cyanine dyes, such as Cy3 and Cy5,[23] thiazole orange exhibits an oxidation potential ($\mathbf{TO}^{+}/\mathbf{TO}^{\cdot 2+}$) of 1.4 eV (vs. NHE).[24] Together with E_{00} = 2.4 eV for **TO**, the excitation is not sufficient for the photooxidation of DNA which stands in contrast to the perylene bisimide dye. The known bioconjugation chemistry of **TO** is versatile. **TO** was linked covalently to the phosphodiester bridges[25] or to 5′-terminal[26] positions of oligonucleotides. Moreover, **TO** was attached synthetically at the terminus of DNA-binding pep-

[a] University of Regensburg, Institute for Organic Chemistry, 93040 Regensburg, Germany
Fax: +49-941-943-4617
E-mail: achim.wagenknecht@chemie.uni-regensburg.de
[b] University of Regensburg, Institute for Pharmacy, 93040 Regensburg, Germany

tides for staining in cell biology and as chemical-biological tools for the investigation of DNA damages that are caused by singlet oxygen.[27–29] **TO** as a base surrogate in PNA was studied extensively in order to detect single base variations in a very sensitive way.[3,30,31] We reported that the emission intensity of **TO** as an artificial DNA base can be modulated by short-range electron transfer.[32] Moreover, we described recently interstrand **TO** dimers in DNA which show a shift of the fluorescence color from the **TO**-typical green (530 nm) to orange (580 nm). This can be used as fluorescence readout for DNA hybridization and for corresponding molecular beacons.[33]

Herein, we describe and compare the optical properties of the **TO** dye and additionally for the derivative **TO3**,[34] as synthetic and fluorescent DNA bases for cell imaging. In comparison to **TO**, the **TO3** chromophore contains an extended carbomethine bridge that shifts the absorption and emission significantly to the red. Both dyes should combine to an interstrand FRET couple that allows monitoring DNA hybridization by an emission color change. In order to study the stacking interactions and the fluorescence properties of the **TO** and the **TO3** dye in a given DNA base sequence we chose our base surrogate approach. The 2′-deoxyribofuranoside moiety of natural nucleotides was replaced by an acyclic linker system that is tethered to the nitrogen either of the thiazole ring or the quinoline ring of the dyes. As previously, (*S*)-1-aminopropane-2,3-diol serves as an acyclic linker between the phosphodiesters. Similar propanediol linkers have been used by others in order to prepare glycol nucleic acids (GNA),[35] twisted intercalating nucleic acids (TINA),[36] alkyne-modified oligonucleotides for the click-type postsynthetic modification,[37–39] and by our group for fluorescent DNA base substitutions by ethidium,[40] indole,[41] perylene bisimide,[20,21] phenothiazine[42] as DNA base surrogates. Avoiding the acid/base labile glycosidic bond of natural nucleosides,[43] the application of a flexible acyclic linker provides a high chemical stability during the preparation of chromophore-DNA conjugates via automated phosphoramidite chemistry, and allows the chromophore to intercalate.

Results and Discussion

For the synthetic incorporation of **TO** into oligonucleotides the (*S*)-1-aminopropane-2,3-diol linker can be attached either to the (i) quinoline nitrogen or (ii) the thiazole nitrogen. The synthesis of the DNA building block and the protocol for automated DNA synthesis for the first alternative modification (**TO-a**) was described recently.[32] The synthesis of the DNA building block for the second alternative modification (**TO-b**)[33] (Scheme 1) starts with the alkylation of the 2-methylbenzotriazole (**1**) with 3-iodopropan-1-ol (**2**) to compound **3**. The subsequent condensation with 1-methylquinolinium iodide (**4**) yields the **TO** derivative **5** in 31%. The reaction proceeds selectively to the *para* position of the methylated quinoline as confirmed by 2D NOESY NMR measurements. Using 1,1′-carbonyldiimidazole, compound **5** was linked by a carbamate function to the enantiomerically pure derivative of (*S*)-1-aminopropane-2,3-diol **6** carrying already the 4,4′-dimethoxytrityl (DMT) protecting group that is needed for the automated DNA phosphoramidite chemistry. The coupling of the phosphiteamide group to the free hydroxy group of **7** was performed using standard procedures in CH_2Cl_2 yielding the phosphoramidite **8**.

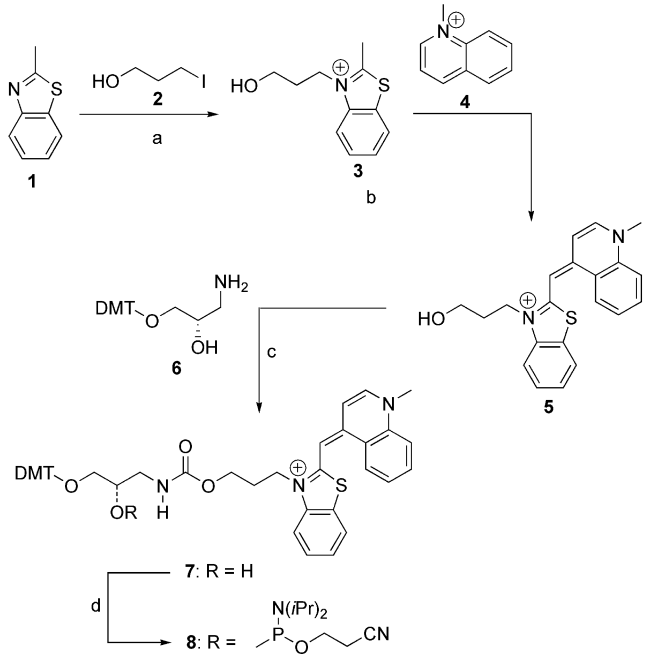

Scheme 1. Synthesis of DNA building block **8** for the **TO-b** modification: a) MeCN, 110 °C, 91 h; 90%; b) NEt_3 (2.5 equiv.), CH_2Cl_2/MeOH = 1:1, room temp., 15 h; 31%; c) 1,1′-carbonyldiimidazole (1.1 equiv.), DMF, room temp., 48 h; 56%; d) DIPEA, 2-cyanoethyl *N*,*N*-diisopropylchlorophosphoramidite, CH_2Cl_2, room temp., 15 h; quant.

Similar to **TO**, the **TO3** chromophore was linked either by the (i) quinoline nitrogen or (ii) the thiazole nitrogen to the linker and the oligonucleotides. For the first structural alternative (**TO3-a**) the key step is the reaction of hydroxypropylated 4-methylquinoline **9**[32] with the hemicyanine **10** (Scheme 2). Best yields (75%) of the dye **11** were only obtained if 3 equiv. of **9** and 6 equiv. of Et_3N were treated with **10**. The remaining reaction steps were similar as described previously for the building block **8**. The coupling with the linker **6** via a carbamate function and subsequent phosphitylation of **12** gave DNA building block **13**.

The attachment of the **TO3** chromophore to oligonucleotides through its thiazole nitrogen started with the reaction of the hydroxypropylated thiazole **3** with *N*,*N*′-diphenylformamidine. The hemicyanine **14** was obtained in 62% yield and subsequently converted with 1,4-dimethylquinolinium iodide (**18**) to the cyanine **15**. The remaining reaction steps were again similar as described previously for the building blocks **8** and **13**: The coupling with the linker **6** via a carbamate function and subsequent phosphitylation of **16** gave DNA building block **17** (Scheme 3).

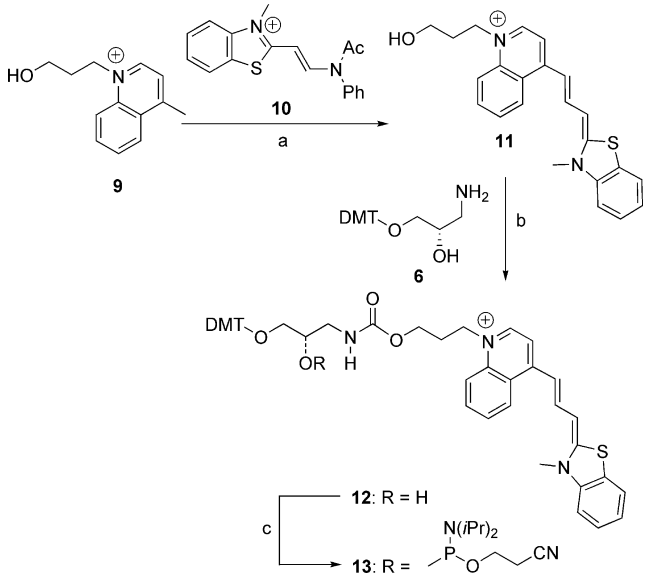

Scheme 2. Synthesis of DNA building block **13** for the **TO3-a** modification: a) Et_3N (6.0 equiv.), CH_2Cl_2, room temp., 48 h; 75%; b) 1,1′-carbonyldiimidazole (2.0 equiv.), DMF, room temp., 13 d, 87%; c) DIPEA, 2-cyanoethyl *N*,*N*-diisopropylchlorophosphoramidite, CH_2Cl_2, room temp., 15 h; quant.

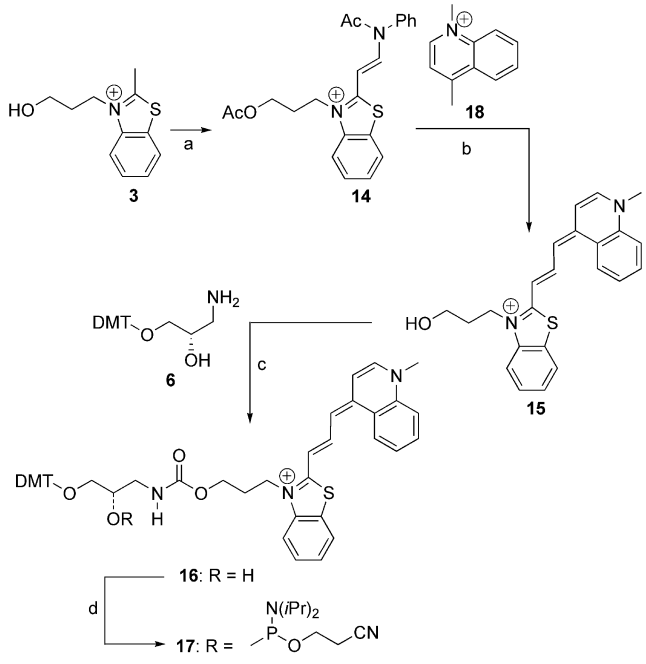

Scheme 3. Synthesis of DNA building block **17** for the **TO3-b** modification: a) *N*,*N*′-diphenylformamidine (1.0 equiv.), Ac_2O, 140 °C, 1 h, 62%; b) 1) Et_3N (6.0 equiv.), CH_2Cl_2, room temp., 72 h, 58%; then 2) MeOH/NH_3(32%) = 2:3, 74 °C, 4 h, 87%; c) 1,1′-carbonyldiimidazole (2.0 equiv.), DMF, room temp., 7 d; 90%; d) DIPEA, 2-cyanoethyl *N*,*N*-diisopropylchlorophosphoramidite, CH_2Cl_2, room temp., overnight.

Using DNA building blocks **8**, **13**, or **17**, the cyanine-modified single-stranded (ss) oligonucleotides were prepared using the DNA synthesizer. The coupling time was extended from 1.6 min (standard) to 61.6 min with an intervening step after 30.8 min for washing and refreshing the activator/phosphoramidite solution in the CPG vial.[40] The corresponding **TO-a**-modified oligonucleotides were prepared according to the literature.[32] The modified single-stranded oligonucleotides were identified by ESI mass spectrometry and quantified by their absorbance at 260 nm using an extinction coefficient of 9.400 $M^{-1}cm^{-1}$ for the **TO-a** and **TO-b** modifications.[3] Duplexes were formed by heating of the modified oligonucleotides to 90 °C (15 min) in the presence of 1.2 equiv. of the corresponding complementary unmodified oligonucleotide strand. For each modification, two duplex sets were synthesized representatively (Scheme 4) in order to study the optical properties of the dyes as artificial DNA base substitutions. Each pair of duplex sets contain the **TO** or **TO3** chromophore in two different environments, either T-A base pairs (e.g. **DNA1C-DNA1G** for the **TO-a** modification) or G-C base pairs (e.g. **DNA4C-DNA4G** for the **TO3-b** modification). Additionally, in each set of duplexes, the base in the complementary strand that sits opposite to the artificial DNA base substitution was varied.

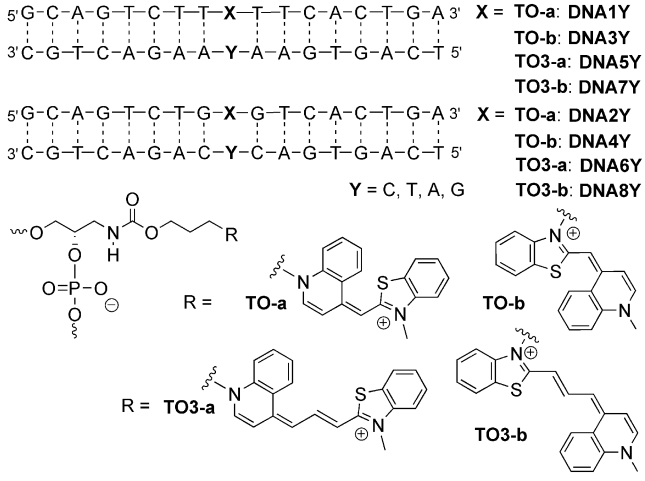

Scheme 4. Sequences of **TO**- and **TO3**-modified DNA duplexes for the investigation of optical properties.

The UV/Vis absorption properties of all **TO**-modified duplexes in the sets **DNA1Y**–**DNA4Y** are remarkably similar showing the presence of the **TO** base surrogate by the characteristic absorption in a range between 450 and 550 nm (Figure 1). The comparison of each **TO** absorption maxima around 505 nm reveals only minor differences in the extinction coefficient. In contrast, a dramatic dependence of the **TO** absorption on the sequential context was described in PNA-DNA hybrids and was interpreted as result of the forced intercalation of the **TO** dye.[3] Hence, the observation of small differences with our **TO**-modified DNA duplexes indicate that the **TO** dyes are not forced to intercalate and tend to bind in the groove. Similar observations were made for the absorption of the **TO3**-type DNA base substitutions in the sets **DNA5Y**–**DNA8Y**. The **TO3** chromophore shows an absorption in a range between 570 and 680 nm with slight variations in the extinction coefficients at the maximum around 645 nm.

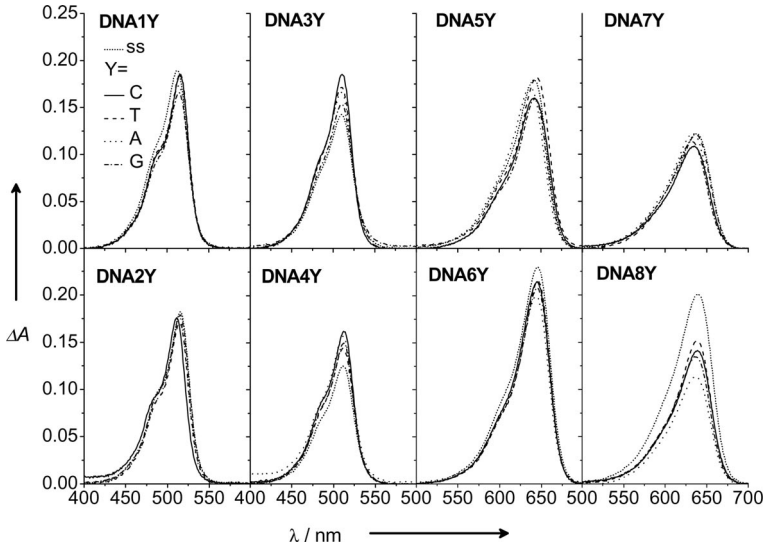

Figure 1. UV/Vis absorption of the duplex sets 2.5 μM **DNA1Y**–**DNA8Y** in 10 mM Na-P_i buffer, 250 mM NaCl, pH 7, ss = single stranded.

In contrast to the UV/Vis absorption spectra, the fluorescence spectra of the **TO**-modified DNA duplexes **DNA1Y**–**DNA4Y** exhibit small differences in the emission quantities depending on the adjacent base pairs (T-A vs. G-C) but significant differences depending on the type of opposite base (C, G, A or T) (Figure 2). Interestingly, the single strands that bear the **TO-a** or **TO-b** modification exhibit similarly strong fluorescence intensities as the corresponding duplexes. This observation indicates a structural preorganization of the **TO** dye with the adjacent bases that exists in the single strand. These interactions reduce the structural flexibility along the methine bridge and hence prevent the radiationless decay of the **TO** dye by internal conversion.[3] Similar results were obtained with the **TO3**-modified duplex sets **DNA5Y**–**DNA8Y**. However, in case of the **TO3** dye both structural variations (adjacent base pairs and opposite base) influence the mode of interaction resulting in different emission quantum yields. This sensitivity of **TO** and the **TO3** chromophores towards its sequential context represents an important observation that can be potentially applied e.g. in time-resolved experiments to study DNA dynamics on short timescales.[44,45]

The melting temperatures (T_m) of the **TO**-modified duplexes **DNA1Y**–**DNA4Y** (Table 1) are remarkably similar within each duplex set, except **DNA2A** and **DNA4A** (which we cannot explain). Representatively, we compared the melting temperatures of the **TO-a**-modified duplexes **DNA1C** and **DNA2C** as well as the **TO-b**-modified duplexes **DNA3C** and **DNA4C** with the corresponding unmodified DNA sequences[41] that bear a standard G instead of the **TO** modifications. This comparison reveals a destabilization in the range of 2.1–5.5 °C, respectively. These values are remarkably small since the incorporation of indole as a base surrogate into oligonucleotides via a similar acyclic linker system resulted in a strong destabilization of the DNA duplexes (approx. –12 °C).[41] Such strong destabilization is typical for single glycol modifications.[35] Obviously, the interactions of the hydrophobic **TO** chromophore with the adjacent bases and base pairs regain some of the lost thermal stability due the glycol linker. This supports the idea that the strong fluorescence that has been observed with all **TO**-modified single strands is the result of a structural preorganization by hydrophobic interactions of **TO** with

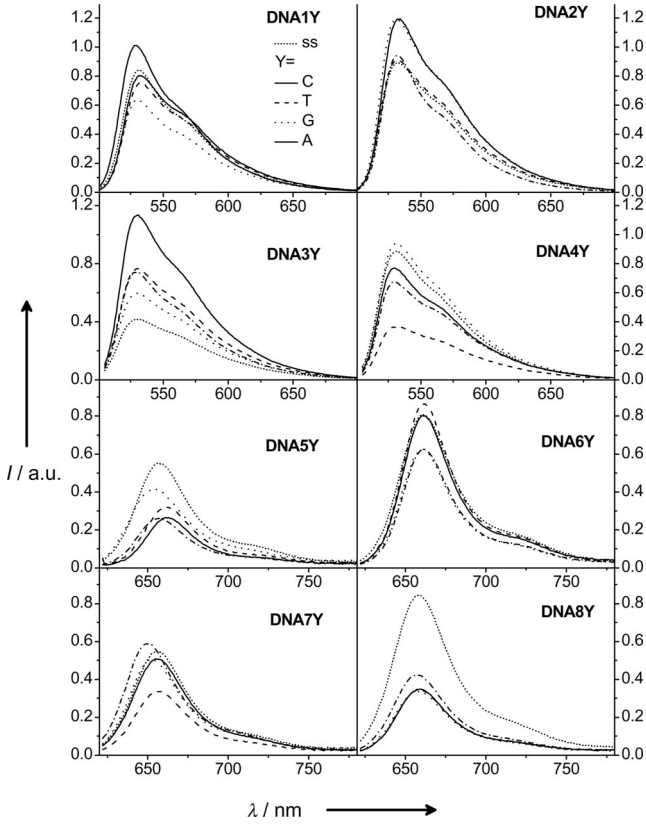

Figure 2. Fluorescence spectra of the duplex sets 2.5 μM **DNA1Y**–**DNA8Y** in 10 mM Na-P_i buffer, 250 mM NaCl, pH 7, ss = single stranded.

the adjacent base pairs. The destabilization of the **TO3-a** and **TO3-b** base substitutions in the duplex sets **DNA5Y**–**DNA8Y** are stronger than the corresponding **TO**-modified counterparts but still lower than typical single glycol modifications. The decrease of the melting temperatures of the representative duplexes **DNA5C**–**DNA8C** are in the range of 3.8–9.1 °C. Obviously, the larger chromophore size in comparison with the **TO** dye influences the duplex stability.

Table 1. Melting temperatures (T_m) and quantum yields ϕ_F of the DNA duplexes, λ = 260 nm, 10–90 °C, interval: 0.7 °C/min, 2.5 μM duplex in 10 mM Na-P_i buffer, 250 mM NaCl, pH 7.

Duplex	Φ_F	T_m (ΔT_m)[a] [°C]	Duplex	Φ_F	T_m (ΔT_m)[a] [°C]
DNA1C	12.4	60.3 (–5.5)	**DNA2C**	7.2	68.4 (–2.3)
DNA1T		59.0	**DNA2T**		67.5
DNA1A		58.0	**DNA2A**		52.2
DNA1G		58.5	**DNA2G**		66.8
DNA3C	16.8	62.0 (–3.8)	**DNA4C**	9.7	68.6 (–2.1)
DNA3T		58.3	**DNA4T**		67.5
DNA3A		58.4	**DNA4A**		48.7
DNA3G		60.5	**DNA4G**		65.9
DNA5C	12.7	56.7 (–9.1)	**DNA6C**	30.5	66.2 (–3.8)
DNA5T		57.7	**DNA6T**		64.2
DNA5A		57.2	**DNA6A**		64.5
DNA5G		57.1	**DNA6G**		64.7
DNA7C	26.2	59.2 (–6.6)	**DNA8C**	16.1	65.7 (–5.0)
DNA7T		58.7	**DNA8T**		64.7
DNA7A		56.9	**DNA8A**		64.7
DNA7G		59.9	**DNA8G**		63.7

[a] Reference duplexes with G instead of **TO-a**, **TO-b**, **TO3-a** or **TO3-b**.

We showed recently that photophysical interaction of two adjacent **TO-b** chromophores as artificial DNA base surrogates alter their optical properties significantly.[33] Intrastrand **TO-b** dimers show strong excitonic interactions that result mainly in fluorescence quenching whereas interstrand **TO-b** dimers exhibit strong excitonic interactions that yield a red-shifted emission. Such results were not obtained with the **TO-a** modification. Hence, interstrand **TO-b** dimers could be regarded as hydrophobically interacting base pairs that stabilize the duplex and exhibit fluorescence color readout for DNA hybridization. The large apparent Stokes' shift of nearly 100 nm together with a brightness that is comparable to a single **TO** label in DNA make the **TO-b** pairs powerful fluorescent labels for live-cell imaging by confocal fluorescence microscopy. Accordingly, we transferred this concept from DNA to RNA, and reported about the optical properties of interstrand **TO-b** dimers in RNA duplexes, and their preliminary application to monitor delivery of RNA to cells.[46]

However, one of the major disadvantages of the optical properties of the **TO-b** dimer in DNA is that the red-shifted fluorescence (580 nm/orange in DNA and 570 nm/yellow in RNA) overlays with parts of the **TO-b** monomer emission (530 nm/green). In the following paragraphs, we describe the interactions of interstrand **TO3** dimers in DNA and how the red-shift can be enhanced by combining the **TO3** modifications with the **TO-b** dye based on an energy transfer process. We synthesized **DNA10**–**DNA14** identical to the published sequences[33] but with the **TO3-a** or **TO3-b** modifications instead of **TO-b**. Additionally, we prepared the **TO-b**-modified **DNA9** and **DNA10** in order to combine them with the **TO3-a**- or **TO3-b**-modified **DNA11**-**DNA14** (Scheme 5).

3' C–A–G–T–C–A–**X**–T–T–G–A–C–G–T–A–C–G 5' **X = TO-b: DNA9; TO3-a: DNA11; TO3-b: DNA13**

5' G–T–C–A–G–T–T–**Y**–A–C–T–G–C–A–T–G–C 3' **Y = TO-b: DNA10; TO3-a: DNA12; TO3-b: DNA14**

5' G–T–C–A–G–T–C–A–A–C–T–G–C–A–T–G–C 3' **DNA15**

Scheme 5. **TO** and **TO3**-modified single-strands **DNA9**-**DNA14** that combine to double modified duplexes (for structures of **TO-b**, **TO3-a** and **TO3-b** see Scheme 4). **DNA15** serves as a reference counterstrand.

The duplexes that are formed of **DNA11** and **DNA12** (**DNA11–12**) and of **DNA13** and **DNA14** (**DNA13–14**) force the two **TO3-a** or **TO3-b** modifications, respectively, into an interstrand interaction similar to the previously published interstrand **TO-b** dimers (**DNA9–10**). The UV/Vis absorption spectra indicate for both duplexes strong excitonic interactions between the **TO3** dyes by an additional absorption band at ca. 585 nm that is not present in the corresponding single **TO3-a**- or **TO3-b**-modified duplexes **DNA11–15** and **DNA13–15**, respectively (Figure 3, left). Such excitonic interactions were also observed in case of the **TO-b**-dimer in DNA that yielded a red-shifted fluorescence maximum.[33] Interestingly, the excitonic interactions between the **TO3** dyes are not reflected by the melting temperatures of the corresponding duplexes (Table 2). The T_m value of both duplexes **DNA11–12** and **DNA13–14** is 60.1 °C which is significantly lower than the corresponding duplex that contains the **TO-b**-dimer (65.5 °C).[33]

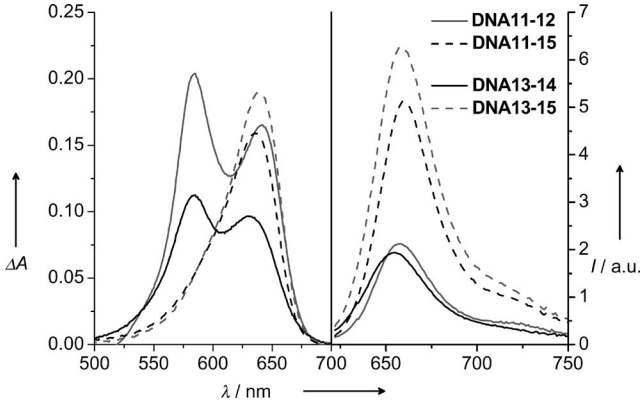

Figure 3. UV/Vis absorption spectra (left) and fluorescence spectra (right) of the double **TO3**-modified duplexes **DNA11–12** and **DNA13–14** in comparison with the single **TO3**-modified **DNA11–15** and **DNA13–15**; 2.5 μM DNA in 10 mM Na-P_i buffer, 250 mM NaCl, pH 7.

However, ground state interactions between two cyanine chromophores do not automatically yield a red-shifted fluorescence. Otherwise, such changes of fluorescence would

Table 2. Melting temperatures 2.5 μM DNA in 10 mM Na-P_i buffer, 250 mM NaCl, pH 7.

Duplex	T_m [°C]	Duplex	T_m (ΔT_m) [°C][a]
DNA9–10	69.4[33]	**DNA9–15**	65.5 (–2.0)[33]
DNA11–12	60.1	**DNA11–15**	62.5
DNA13–14	60.1	**DNA13–15**	62.2 (–5.5)
DNA11–10	57.5	**DNA13–10**	66.7
DNA9–12	58.7	**DNA9–14**	67.7

[a] The corresponding unmodified DNA duplex that contains G instead of **TO-b**, **TO3-a** or **TO3-b** shows T_m = 67.5 °C.

have been detected previously with **TO** dimer conjugates (like **TOTO**).[47,48] Unfortunately, this is also true for the **TO3-a** dimer in **DNA11–12** as well as the **TO3-b** dimer in **DNA13–14** (Figure 3, right): When excited at 620 nm, both duplexes exhibit a significant fluorescence quenching compared to the single-labeled references **DNA11–15** and **DNA13–15**, a typical result of chromophore aggregation.

The emission of the **TO** dye (520–600 nm) overlaps pretty well with the absorption of the **TO3** dye (550–650). By combining the **TO** and the **TO3** chromophores that are placed in two different strands a fluorescence resonance energy transfer (FRET) process could only occur in the hybridized duplex. Accordingly we combined the **TO-b** modification of **DNA9** and **DNA10** with the **TO3-a** modification yielding **DNA9–12** and **DNA11–10**, and with the **TO3-b** modification yielding **DNA9–14** and **DNA13–10**. These double modified duplexes show all the typical absorption band of both, the **TO** and the **TO3** dyes, excluding a groundstate interaction between them (Figure 4, top). When excited at 490 nm (the **TO**-typical wavelength) all duplexes exhibit an additional emission at 660–670 nm (the **TO3**-typical range) which is the result of a FRET-type process (Figure 4, bottom).

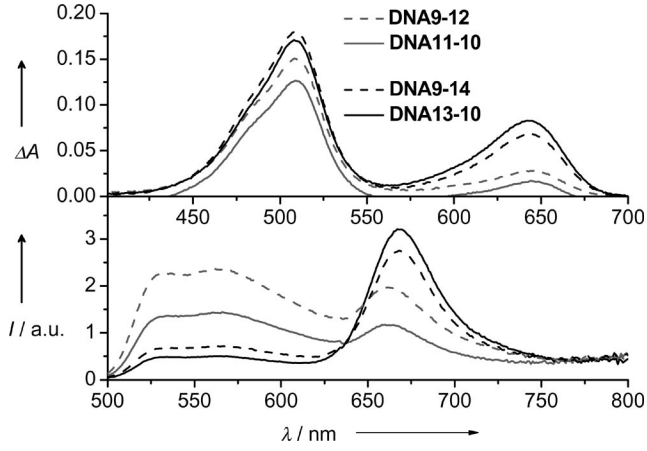

Figure 4. UV/Vis absorption spectra (top) and fluorescence spectra (bottom) of the double **TO/TO3**-modified duplexes **DNA9–12**, **DNA9–14**, **DNA11–10** and **DNA 13–10**; 2.5 μM DNA in 10 mM Na-P_i buffer, 250 mM NaCl, pH 7, excitation at 490 nm.

Interestingly, the FRET efficiency differs significantly between the duplexes. Both dye combinations with the **TO3-a** modification (**DNA9–12** and **DNA11–10**) exhibit a fluorescence intensity of the **TO3** dye that is smaller than the remaining **TO** emission (ratio I_{668nm}/I_{531nm} = 0.8 or 0.9, respectively) indicating a low FRET efficiency (Figure 5), right. On the other hand, in case of the duplexes that bear the **TO3-b** chromophore in combination with the **TO-b** dye (**DNA9–14** and **DNA13–10**) the FRET efficiency is high and the **TO** emission is significantly reduced (ratio I_{668nm}/I_{531nm} = 4.1 and 6.7, respectively). It is important to note that the observed FRET efficiencies correlate with the melting temperatures (Table 2). For instance, if the counterstrands of **DNA9–12** or **DNA9–14**, respectively, would exchange inside the cells by unmodified counterparts, duplex **DNA9–15** would be the result (T_m of 65.5 °C). That means, **DNA9–12** would exchange to **DNA9–15** whereas **DNA9–14** would not. Obviously, the interstrand chromophore orientation of **TO-b** in the **TO3-b**-modified duplexes **DNA9–14** and **DNA13–10** is more suitable for an efficient FRET compared to the **TO3-a**-modified duplexes **DNA9–12** and **DNA11–10**. In both duplexes, **DNA9–14** and **DNA13–10**, the melting temperature can be also obtained by temperature-dependent fluorescence spectroscopy (Figure 5, left) as the FRET efficiency drops at the same temperature as the cooperative dehybridization.

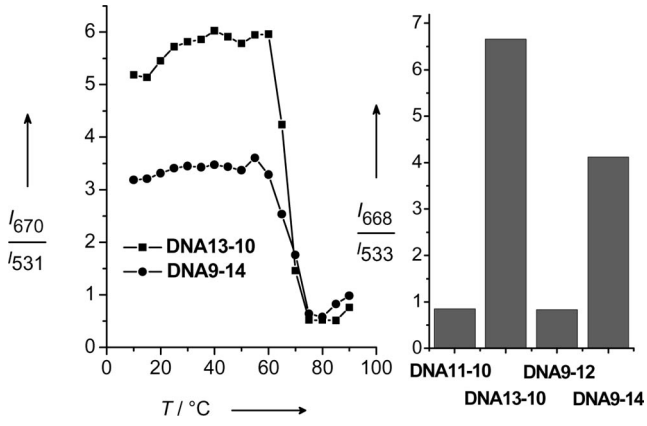

Figure 5. Temperature-dependent fluorescence (left) and fluorescence intensity ratios at 20 °C (right) of **TO/TO3**-modified duplexes **DNA9–12**, **DNA9–14**, **DNA11–10** and **DNA 13–10**; 2.5 μM DNA in 10 mM Na-P_i buffer, 250 mM NaCl, pH 7, excitation at 490 nm.

To evaluate these DNA duplexes for potential biological applications, CHO-K1 cells were microinjected representatively with **DNA13–10**, the duplex that exhibits the best FRET efficiency between **TO** and **TO3**. The fluorescence emission of DNA inside cells was recorded with a bandpass filter from 530 to 600 nm (green channel) and a longpass filter of 650 nm (red channel) (Figure 6, top). Remarkably, the difference in the fluorescence emission persisted even inside cells. The ratio of the fluorescence intensity of the red to the green channel was 1.85 ± 0.23 (in comparison to 0.34 ± 0.09 for the single **TO** modification in the single stranded **DNA9** in Figure 6, bottom).

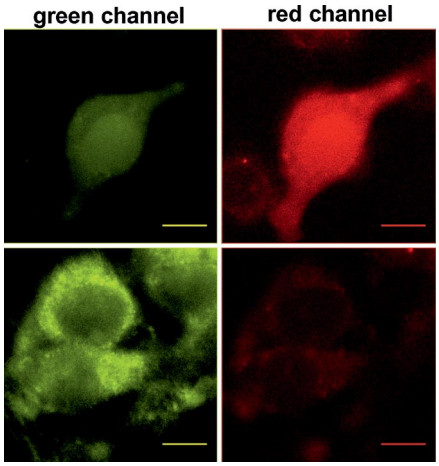

Figure 6. CHO-K1 cells were microinjected with **DNA13–10** (top) and **DNA9** (bottom) and thereafter imaged for fluorescence emission from 530–600 nm (green channel) and >650 nm (red channel) by confocal laser scanning microscopy. Bars indicate 10 μm.

Conclusions

The **TO** and the **TO3** dyes as fluorescent DNA base substitutions show a brightness that is sufficient for bioanalytic and imaging applications. In contrast to the non-covalently binding **TO**-PRO3 **TOTO** and **TOTO3** dyes,[49] the **TO**- and **TO3**-modified oligonucleotides should potentially be cell-permeable. Thus, **TO** and **TO3** represent promising internal fluorescence labels for DNA and RNA. A DNA hybridization-dependent energy transfer process can be obtained between the **TO** and **TO3** modifications if they are placed in two complementary strands. As a result, the emission is shifted from the **TO**-typical value of 530 nm to 670 nm. This concept can be applied for fluorescence imaging to monitor DNA and RNA delivery as well as processing inside living cells by confocal microscopy.

Experimental Section

Materials and Methods: Chemicals were purchased from Aldrich, Alfa Aesar and Merck. Unmodified oligonucleotides were purchased from Metabion. T.l.c. was performed on Fluka silica gel 60 F254 coated aluminum foil. Flash chromatography was carried out with silica gel 60 from Aldrich (60–43 μm). Spectroscopic measurements were recorded in Na-Pi buffer solution (10 mM) using quartz-glass cuvettes (10 mm). Absorption spectra and the melting temperatures (2.5 μM DNA, 250 mM NaCl, 10–90 °C, 0.7 °C/min, step width 1 °C) were recorded with a Varian Cary 100 spectrometer equipped with a 6 × 6 cell changer unit. Fluorescence was measured with a Jobin–Yvon Fluoromax 3 fluorimeter with a step width of 1 nm and an integration time of 0.2 s. All spectra were recorded with an excitation and emission bandpass of 2 nm and are corrected for Raman emission from the buffer solution.

Synthesis of Compound 3: Under nitrogen, 2-methylbenzothiazole (**1**, 13.7 mL, 107.5 mmol) and 3-iodo-1-propanol (**2**, 10.0 g, 53.8 mmol) were dissolved in 30 mL acetonitrile. The mixture was stirred under reflux for 91 h, then cooled to room temp. and kept in the fridge overnight. The precipitate was collected and washed three times with 15 mL cold Et_2O, dried under reduced pressure. A white solid was yielded (90.0%). ^{1}H NMR (300 MHz, [D_6]-DMSO): δ = 8.46–8.29 (m, 2 H, arom.), 7.93–7.78 (m, 2 H, arom.), 4.83 (m, 1 H, OH), 4.78 (t, J = 7.4 Hz, 2 H, NCH_2-), 3.53 (m, 2 H, -CH_2-O), 3.22 (s, 3 H, Me), 2.06 (m, 2 H, -CH_2-) ppm. ^{13}C NMR (125.8 MHz, [D_6]DMSO): δ = 177.2, 140.8, 129.3, 129.0, 128.0, 124.6, 116.7 (benzothiazole arom.), 57.28, 45.78, 30.35 (propyl), 16.70 (2-Me) ppm. MS (ESI): m/z (%) = 208.1 (100) $[M]^+$. HR-MS (FAB): found: m/z = 208.0801 $[M]^+$, calcd. 208.0791.

Synthesis of Compound 5: Under nitrogen **3** (1.17 g, 3.5 mmol) and *N*-methylquinoline (**4**, 1.14 g, 4.2 mmol) were dissolved in 20 mL CH_2Cl_2/MeOH (1:1 v:v). Dry Et_3N (1.2 mL, 8.6 mmol) was added yielding in an immediate deep red color. The reaction mixture was stirred under reflux overnight, then cooled to room temp. The product was collected and washed three times with 15 mL cold Et_2O and dried under reduced pressure (31%). ^{1}H NMR (300 MHz, [D_6]DMSO): δ = 8.75 (m, 1 H, arom.), 8.43 (m, 1 H, arom.), 8.09–7.99 (m, 3 H, arom.), 7.79–7.74 (m, 2 H, arom.) 7.64–7.58 (m, 1 H, arom.), 7.44–7.37 (m, 2 H, arom.), 7.05 (s, 1 H, olefin-H), 5.05 (t, J = 4.67 Hz, 1 H, OH), 4.63 (m, 2 H, N-CH_2-), 4.18 (s, 3 H, N-Me), 3.58 (m, 2 H, -CH_2-O), 2.00 (m, 2 H, -CH_2-) ppm. ^{13}C NMR (125.8 MHz, [D_6]DMSO): δ = 159.2, 148.6, 145.0, 139.9, 138.0, 133.1, 128.1, 126.9, 125.2, 124.4, 124.0, 123.8, 122.9, 118.2, 112.7, 107.8, 87.4 (thiazole orange), 57.3 (propyl), 45.6 (N-Me), 42.3, 30.1 (propyl) ppm. MS (ESI): m/z (%) = 349.0 (100) $[M]^+$. HR-MS (FAB): found: m/z = 349.1380 $[M]^+$, calcd. 349.1375.

Synthesis of Compound 7: 5 (434 mg, 0.911 mmol) was dissolved in 5 mL DMF and 1,1′-carbonyldiimidazole (195 mg, 1 mmol) was added. The solution was stirred at room temp. for 3 h. [3-(4,4′-Dimethoxytrityl)-2-hydroxypropyl]amine (**6**, 395 mg, 1 mmol) was added and the solution was stirred for 48 h and the solvents evaporated to dryness. The crude product was purified by flash chromatography (silica gel) with a gradient of MeOH in CH_2Cl_2 (0–5%) yielding a dark red solid (56%). T.l.c. (CH_2Cl_2/MeOH, 9:1) R_f = 0.4. ^{1}H NMR (300 MHz, [D_6]DMSO): δ = 8.75 (m, 1 H, arom ppm. **TO**), 8.64 (m, 1 H, arom. **TO**), 8.09–7.96 (m, 3 H, arom. **TO**), 7.80–7.68 (m, 2 H, arom. **TO**), 7.59 (m, 1 H, arom. **TO**), 7.37 (m, 2 H, arom. **TO**), 7.34 (m, 2 H, arom. DMT), 7.23 (m, 7 H, arom. DMT), 6.92–6.84 (m, 4 H, arom. DMT), 4.98 (d, 1 H, J = 5.22, OH), 4.64 (m, 2 H, N-CH_2-), 4.19 (s, 3 H, N-Me), 4.10 (m, 2 H, -CH_2-O), 3.73 (s, 1 H, -CH-OH), 3.70 (s, 6 H, 2 × OMe), 3.33 (s, 1 H, NH), 3.30 (m, 1 H, NH-CH_2-), 3.16 (m, 1 H, NH-CH_2-), 2.96 (m, 1 H, -CH_2-ODMT), 2.86 (m, 1 H, -CH_2-ODMT), 2.09 (m, 2 H, -CH_2-) ppm. ^{13}C NMR (125.8 MHz, [D_6]DMSO): δ = 166.8, 157.9, 148.8, 145.0, 139.8, 137.9, 135.6, 133.0, 131.5, 130.2, 129.6, 128.6, 128.3, 127.6, 126.9, 126.4, 123.8, 112.9, 85.1 [O-C-(PhOMe)$_2$Ph], 68.6, 65.6 (CH_2O), 54.9 (OMe), 42.4 (propyl), 28.8 (propyl) ppm. MS (ESI): m/z (%) = 768.3 (100) $[M]^+$. HR-MS (FAB): found: m/z = 768.3096 $[M]^+$, calcd. 768.3107. MS (MALDI-**TO**F): found: m/z = 768.2 $[M]^+$, calcd. 768.3.

Synthesis of DNA Building Block 8: Under nitrogen **7** (60 mg, 0.067 mmol) was dissolved in 4 mL dry CH_2Cl_2. Dry diisopropylamine (35 μL, 0.2 mmol) and 2-cyanoethyl *N*,*N*-diisopropylchlorophosphoramidite (21 μL, 0.094 mmol) was added. The reaction mixture was stirred overnight at room temp. and subsequently washed by freshly prepared satd. aq. $NaHCO_3$, dried with Na_2SO_4, and the solvents evaporated to dryness. The resulting dark red solid was solved in dry MeCN (0.6 mL) and applied directly for automated DNA synthesis. T.l.c. R_f (CH_2Cl_2/MeOH = 9:1) = 0.5. ^{31}P NMR (121 MHz, DMSO): δ = 149.59, 149.06 ppm. MS (ESI): m/z (%) = 968.6 (100) $[M]^+$.

Synthesis of Compound 11: Under nitrogen, **10** (1.75 g, 4 mmol) and **9** (3.95 g, 12 mmol) were dissolved in dry DCM (25 mL) and

3.30 mL dry triethylamine (24 mmol) were added slowly. After the mixture was stirred for 2 d at room temp., the resulting precipitate was collected by filtration under reduced pressure and washed with diethyl ether (3 × 10 mL) and methanol (3 × 5 mL). The obtained solid was recrystallized from DCM/MeOH = 10:1 to afford **11** as a green solid product (1.55 g, 75%). ^{1}H NMR (600 MHz; [D$_6$]-DMSO): δ = 1.96 (quint, 2 H, -CH$_2$-), 3.69 (s, 3 H, N-Me), 3.48 (q, 2 H, -CH$_2$-OH), 4.56 (t, 2 H, N-CH$_2$-), 4.77 (t, 1 H, OH), 6.46 (d, 1 H, trimethine-H), 7.06 (d, 1 H, trimethine-H), 7.24 (t, 1 H, arom.), 7.42 (t, 1 H, arom.), 7.52 (d, 1 H, arom.), 7.66 (t, 1 H, arom.), 7.78 (d, 1 H, arom.), 7.83, (d, 1 H, arom.), 7.91 (t, 1 H, arom.), 8.02 (d, 1 H, arom.), 8.09 (t, 1 H, trimethine-H), 8.32 (d, 1 H, arom.), 8.41 (d, 1 H, arom.) ppm. ^{13}C NMR (600 MHz; [D$_6$]-DMSO): δ = 31.6 (propyl), 32.8 (N-Me6), 51.4 (propyl), 57.6 (propyl),98.7, 109.2, 109.5, 112.4, 117.7, 122.5, 124.0, 124.3, 124.6, 125.1, 126.5, 127.5, 133.2, 137.8, 141.9, 142.3, 143.7, 150.3, 161.6 ppm. ESI-MS: *m*/*z* (%) = 375.0 (100) [M$^+$]. HR-MS (FAB): found: *m*/*z* = 375.1532 [M]$^+$, calcd. 375.1526.

Synthesis of Compound 12: Under nitrogen, **11** (0.5 g, 1.0 mmol) was dissolved in 40 mL dry DMF and 1,1′-carbodiimidazole (0.33 g, 2 mmol) was added. After stirring at room temperature for 6 d, **6** (0.78 g, 2 mmol) was added and again stirred for 7 d at room temp. The solvent was then removed under reduced pressure and the resulting solid purified by flash-column-chromatography (SiO$_2$, DCM/MeOH, 10:1 + 10% pyridine). Compound **12** was obtained as a blue solid (0.80 g, 87%). T.l.c. (DCM/MeOH, 10:1) R_f = 0.38. ^{1}H NMR (300 MHz; [D$_6$]DMSO): δ = 2.08–2.12 (m, 2 H, -CH$_2$-), 2.83–2.86 and 2.88–2.92 (m, 1 H, -CH$_2$-ODMT), 2.95–2.99 and 3.15–3.24 (m 1 H, NH-CH$_2$-), 3.70 (s, 6 H, 2 × OMe), 3.74 (s, 1 H, -CH-OH), 3.97–4.01 (t, 2 H, -CH$_2$-O), 4.55–4.59 (t, 2 H, N-CH$_2$-), 4.98 (d, 1 H, OH), 6.51 (d, 1 H, **TO**-3), 6.86 (d, 4 H, arom. DMT), 7.01 (t, 1 H, **TO**-3), 7.11 (m, 1 H, **TO**-3), 7.23–7.26 (m, 7 H, arom. DMT), 7.50 (t, 1 H, **TO**-3 arom.), 7.61 (d, 1 H, **TO**-3 arom.), 7.70 (t, 1 H, **TO**-3 arom.), 7.84–7-89 (m, 2 H, **TO**-3 arom.), 7.95–7.96 (m, 1 H, **TO**-3 arom.), 8.02–8.05 (m, 1 H, **TO**-3 arom.), 8.18 (t, 1 H, **TO**-3), 8.33 (d, 1 H, **TO**-3 arom.), 8.47 (d, 1 H, **TO**-3 arom.) ppm. ^{13}C NMR (600 MHz; [D$_6$]DMSO): δ = 28.3, 30.7, 32.9, 35.7, 44.2, 54.9, 60.5, 65.6, 68.7, 85.1, 99.1, 108.2, 109.2, 112.6, 113.0, 114.9, 115.9, 117.6, 122.5, 123.8, 124.2, 124.6, 125.2, 126.5, 127.6, 129.6, 133.4, 135.7, 137.8, 141.9, 145.0, 156.0, 157.9, 162.2 ppm. ESI-MS: *m*/*z* (%) = 794.2 (100) [M$^+$]. HR-MS (FAB): found: *m*/*z* = 794.3270 [M]$^+$, calcd. 794.3258.

Synthesis of DNA Building Block 13: Under argon, **12** (0.3 g, 0.33 mmol) and dry 166 μL DIPEA (0.97 mmol) were dissolved in 10 mL dry DCM. Then, 125 μL 2-cyanoethyl *N*,*N*-diisopropylchlorophosphoramidite (0.56 mmol) were added, the mixture was stirred at room temperature for 16 h. After complete reaction, the organic phase was washed with a satd. aq. NaHCO$_3$, dried with Na$_2$SO$_4$ and the solvents evaporated to dryness. The resulting dark blue solid was solved in dry MeCN (3.5 mL) and applied directly for automated DNA synthesis. T.l.c. R_f (CH$_2$Cl$_2$/acetone = 2:1) = 0.3. ^{31}P NMR (121 MHz, DMSO): δ = 150.06, 149.70 ppm.

Synthesis of Compound 14: Compound **3** (3.31 g, 9.8 mmol) in dry acetic anhydride (30 mL) was refluxed until completely dissolved. Afterwards, *N*,*N*-diphenylformamidine (1.93 g, 9.8 mmol) was added and refluxed again for 1 h. The mixture was cooled to room temp. and 40 mL diethyl ether were added slowly. After the resulting oil has been separated and dried under reduced pressure for 24 h, it was resolved in DCM and washed with water (4 ×). 2.9 g of a dark red oil **14** were obtained (62%). Unfortunatly, the purification of this compound was never sufficient to provide all analytical data. ^{1}H NMR (300 MHz; [D$_6$]DMSO): δ = 1.79 (m, 3 H, O-acetyl-CH$_3$), 1.92–1.98 (m, 2 H, -CH$_2$), 2.06 (s, 3 H, *N*-acetyl-CH$_3$), 3.93 (t, 2 H, O-CH$_2$-), 4.49 (t, 2 H, N-CH$_2$-), 5.67 (d, 1 H, methin-H), 7.52–7.57 (m, 2 H, benzothiazol arom.), 7.63–7.81 (m, 5 H, arom.), 8.17 (d, 1 H, benzothiazol arom.), 8.33 (dd, 1 H, benzothiazol arom.), 8.84 (d, 1 H, methine-H) ppm. ESI-MS: *m*/*z* (%) = 394.9 (84) [M$^+$].

Synthesis of Compound 15: 1) Under nitrogen, **14** (1.0 g, 2 mmol) and **4** (0.57 g, 2 mmol) were dissolved in 20 mL dry DCM and 1.66 mL dry triethylamine (12 mmol) were added slowly. After the mixture was stirred for 3 d at room temperature, the resulting precipitate was collected by filtration under reduced pressure to afford a dark blue solid (0.63 g, 58%). 2) The obtained blue solid was dissolved in 25 mL of MeOH/NM$_3$ (32%) = 2:3 and refluxed for 4 h. The resulting product was collected by filtration under reduced pressure and washed with dry DCM (2 × 5 mL) to afford **15** as a dark green solid (0.51 g, 87%). ^{1}H NMR (600 MHz; [D$_6$]DMSO): δ = 1.88 (quint, 2 H, -CH$_2$-), 3.54 (q, 2 H, -CH$_2$-O), 4.13 (s, 3 H, N-Me), 4.25 (t, 2 H, N-CH$_2$), 4.83 (t, 1 H, OH), 6.49 (d, 1 H, trimethine-H), 7.09 (d, 1 H, trimethine-H), 7.27 (t, 1 H, arom.), 7.45 (t, 1 H, arom.), 7.52 (d, 1 H, arom.), 7.70 (m, 1 H, arom.), 7.82 (m, 1 H, arom.), 7.83 (d, 1 H, arom.), 7.96 (m, 1 H, arom.), 7.97 (m, 1 H, arom.), 8.11 (t, 1 H, trimethine-H), 8.38 (d, 1 H, arom.), 8.45 (d, 1 H, arom.) ppm. ^{13}C NMR (600 MHz; [D$_6$]-DMSO): δ = 30.0 (propyl), 42.2 (**TO3**), 42.9 (propyl), 57.6 (propyl), 98.2, 109.5, 109.3, 112.2, 117.9, 122.4, 123.9, 124.0, 124.6, 124.8, 126.7, 127.5, 133.2, 138.8, 141.5, 143.2, 143.6, 150.4, 160.7 ppm. ESI-MS**:** *m*/*z* (%) = 375.0 (100) [M$^+$]. HR-MS (FAB): found: *m*/*z* = 375.1524 [M]$^+$, calcd. 375.1526.

Synthesis of Compound 16: Under nitrogen, **15** (0.5 g, 1.0 mmol) was dissolved in 40 mL dry DMF and 0.33 g 1,1′-carbodiimidazole (2 mmol) were added. After stirring at room temp. for 2 d, **6** (0.78 g, 2 mmol) was added and again stirred for 2 d at room temp. The solvent was then removed under reduced pressure and the resulting solid purified by flash-column chromatography (SiO$_2$, DCM/MeOH, 10:1 + 10% pyridine). Compound **16** was obtained as a blue solid (0.83 g, 90%). T.l.c. (DCM/MeOH, 10:1) R_f = 0.38. ^{1}H NMR (300 MHz; [D$_6$]DMSO): δ = 1.99–2.03 (m, 2 H, -CH$_2$-), 2.88–2.99 (m, 2 H, CH$_2$-ODMT), 3.18–3.26 (m, 2 H, NH-CH$_2$), 3.33 (s, 1 H, NH), 3.70 (s, 6 H, 2 × OMe), 3.73 (s, 1 H, -CH-OH), 5.02 (d, 1 H, OH), 6.47 (d, 1 H, methine-H), 6.84 (m, 4 H, arom. DMT), 7.08–7.13 (m 1 H, **TO**-3), 7.20–7.24 (m, 7 H, arom. DMT), 7.26–7.32 (m 2 H, **TO**-3 arom.), 7.43–7.56 (m, 2 H, **TO**-3 arom.), 7.64–7.69 (m, 1 H, **TO**-3 arom.), 7.85–7.90 (m, 2 H, **TO**-3 arom.), 7.93–8.02 (m, 3 H, **TO**-3 arom.), 8.10–8.18 (m 1 H, **TO**-3) ppm. ^{13}C NMR (400 MHz; [D$_6$]DMSO): δ = 26.5, 30.7, 35.7, 42.2, 44.3, 54.9, 65.6, 68.7, 85.1, 98.0, 109.5, 109.8, 112.1, 113.0, 118.1, 122.5, 123.8, 124.0, 124.6, 126.4, 127.6, 129.6, 133.3, 135.7, 138.1, 141.3, 143.4, 145.0, 157.9, 162.2 ppm. ESI-MS**:** *m*/*z* (%) = 794.2 (100) [M$^+$]. HR-MS (FAB): found: *m*/*z* = 794.3242 [M]$^+$, calcd. 794.3258.

Synthesis of DNA Building Block 17: Under argon, **16** (0.3 g, 0.33 mmol) and 166 μL dry DIPEA (0.97 mmol) were dissolved in 10 mL dry DCM. After 125 μL 2-cyanoethyl *N*,*N*-diisopropylchlorophosphoramidite (0.56 mmol) were added, the reaction mixture was stirred at room temp. for 16 h. After complete reaction, the organic phase was washed with satd. aq. NaHCO$_3$, dried with Na$_2$SO$_4$ and the solvents evaporated to dryness. The resulting dark blue solid was solved in dry MeCN (3.5 mL) and applied directly for automated DNA synthesis. T.l.c. R_f (CH$_2$Cl$_2$/acetone = 2:1) = 0.3. ^{31}P NMR (121 MHz, DMSO): δ = 150.06, 149.70 ppm.

Preparation of DNA: Oligonucleotides were prepared with an Expedite 8909 Synthesizer from Applied Biosystems (ABI) using standard phosphoramidite chemistry. Reagents and CPG (1 μmol) were

purchased from ABI and Glen Research. The synthesis of thiazole orange-modified as well as trimethine thiazole orange-modified DNA oligonucleotides was performed using a modified protocol. Activator solution (0.45 M tetrazole in acetonitrile) was pumped simultaneously with the building block (0.1 M in acetonitrile). The coupling time was extended to 61 min with an intervening step after 30.8 min for washing and refreshing the activator/phosphoramidite solution in the CPG vial. The CPG vial was flushed with dry acetonitrile after the coupling. After preparation, the trityl-off oligonucleotide was cleaved from the resin and deprotected by treatment with conc. NH_4OH at room temperature overnight. The modified oligonucleotides were purified by HPLC on a semipreparative RP-C18 column (300 Å, Supelco) using the following conditions: A = NH_4OAc buffer (50 mM), pH = 6.5; B = acetonitrile; gradient 0–20% B over 70 min for **TO** and 50 min for **TO3**, flow rate 2.5 mL/min, UV/Vis detection at 260 and 512 nm for **TO**-modified oligonucleotides, 260 and 600 nm for **TO3**-modified oligonucleotides. The oligonucleotides were lyophilized and quantified by their absorbance in 10 mM NaP_i buffer at 260 nm on a Varian Cary 100 spectrometer. The following total yields range from 3% to 16% depending on the sequential context. Duplexes were formed by heating to 90 °C (15 min.) followed by slow cooling.

Microinjection and Confocal Laser Scanning Microscopy: CHO-K1 cells were seeded one day prior microinjection on glass coverslips. Glass capillaries were loaded with 100 μM DNA solutions. The microinjection was performed using an InjectMan in combination with a microinjector FemtoJet (Eppendorf) coupled to a Axiovert 200 fluorescence microscope (Carl Zeiss). The injection pressure was ca. 120 hPa and the injection time per cell was 0.3 s. After injection, the culture medium (Ham's F12 containing 10% serum) was changed and the cells were imaged using a Zeiss Axiovert 200 M microscope coupled to a Zeiss LSM 510 scanning device (Carl Zeiss). After excitation with 488 and 514 nm the fluorescence was detected using a 530–600 nm band-pass filter (green channel) and a 560 nm longpass filter (red channel). The ratio of the red to green fluorescence was calculated using the Image J software.

Acknowledgments

This work was supported by the Deutsche Forschungsgemeinschaft (DFG) (Wa 1386/9) and the University of Regensburg.

[1] a) S. Tyagi, F. R. Kramer, *Nat. Biotechnol.* **1996**, *14*, 303–308; b) T. Heyduk, E. Heyduk, *Nat. Biotechnol.* **2002**, *20*, 171–176; c) M. K. Johansson, R. M. Cook, *Chem. Eur. J.* **2003**, *9*, 3466–3471; d) W. Tan, K. Wang, T. J. Drake, *Curr. Opin. Chem. Biol.* **2004**, *8*, 547–553.

[2] a) K. Nakatani, *ChemBioChem* **2004**, *5*, 1623–1633; b) R. T. Ranasinghe, T. Brown, *Chem. Commun.* **2005**, 5487–5502; c) M. Strerath, A. Marx, *Angew. Chem. Int. Ed.* **2005**, *44*, 7842–7849.

[3] a) O. Köhler, D. V. Jarikote, O. Seitz, *ChemBioChem* **2005**, *6*, 69–77; b) D. V. Jarikote, N. Krebs, S. Tannert, B. Röder, O. Seitz, *Chem. Eur. J.* **2007**, *13*, 300–310; c) E. Socher, D. V. Jarikote, A. Knoll, L. Röglin, J. Burmeister, O. Seitz, *Anal. Biochem.* **2008**, *375*, 318–330.

[4] A. Okamoto, K. Tainaka, Y. Ochi, K. Kanatami, I. Saito, *Mol. Biosyst.* **2006**, *2*, 122–127.

[5] B. Venkatesan, Y. J. Seo, B. H. Kim, *Chem. Soc. Rev.* **2008**, *37*, 648–663.

[6] L. G. Kostrikis, S. Tyagi, M. M. Mhlanga, D. D. Ho, F. R. Kramer, *Science* **1998**, *279*, 1228–1229.

[7] S. S.-M. Sum, D. K.-H. Wong, M.-F. Yuen, H.-J. Yuan, J. Yu, C.-L. Lai, D. Ho, L. Zhang, *J. Clin. Microbiol.* **2004**, *42*, 3438–3440.

[8] D. P. Bratu, B.-J. Cha, M. M. Mhlanga, F. R. Kramer, S. Tyagi, *Proc. Natl. Acad. Sci. USA* **2003**, *100*, 13308–13313.

[9] K. Wang, Z. Tang, C. J. Yang, Y. Kim, X. Fang, W. Li, Y. Wu, C. D. Medley, Z. Cao, J. Li, P. Colon, H. Lin, W. Tan, *Angew. Chem. Int. Ed.* **2009**, *48*, 856–870.

[10] a) S. Tyagi, S. A. E. Marras, F. R. Kramer, *Nat. Biotechnol.* **2000**, *18*, 1191–1196; b) J. R. Epstein, I. Biran, D. R. Walt, *Anal. Chim. Acta* **2002**, *469*, 3–36; c) A. A. Marti, S. Jockusch, N. Stevens, J. Ju, N. J. Turro, *Acc. Chem. Res.* **2007**, *40*, 402–409.

[11] H. Kashida, H. Asanuma, M. Komiyama, *Chem. Commun.* **2006**, 2768–2770.

[12] a) I. Trkulja, R. Häner, *J. Am. Chem. Soc.* **2007**, *129*, 7982–7989; b) V. L. Malinovskii, F. Samain, R. Häner, *Angew. Chem. Int. Ed.* **2007**, *46*, 4464–4467.

[13] K. V. Balakin, V. A. Korshun, I. I. Mikhalev, G. V. Maleev, A. D. Malakhov, I. A. Prokhorenko, Y. A. Berlin, *Biosens. Bioelectron.* **1998**, *13*, 771–778.

[14] a) K. Yamana, T. Iwai, Y. Ohtani, S. Sato, M. Nakamura, H. Nakano, *Bioconjugate Chem.* **2002**, *13*, 1266–1273; b) K. Yamana, Y. Fukunaga, Y. Ohtani, S. Sato, M. Nakamura, W. J. Kim, T. Akaike, A. Maruyama, *Chem. Commun.* **2005**, 2509–2511.

[15] K. Seio, M. Mizuta, K. Tasaki, K. Tamaki, A. Ohkubo, M. Sekine, *Bioorg. Med. Chem.* **2008**, *16*, 8287–8293.

[16] K. Fujimoto, H. Shimizu, M. Inouye, *J. Org. Chem.* **2004**, *69*, 3271–3275.

[17] Y. Chen, C. J. Yang, Y. Wu, P. Conlon, Y. Kim, H. Lin, W. Tan, *ChemBioChem* **2008**, *9*, 355–359.

[18] P. Conlon, C. J. Yang, Y. Wu, Y. Chen, K. Martinez, Y. Kim, N. Stevens, A. A. Marti, S. Jockusch, N. J. Turro, W. Tan, *J. Am. Chem. Soc.* **2008**, *130*, 336–342.

[19] H. Kashida, T. Takatsu, T. Fujii, K. Sekiguchi, X. Liang, K. Niwa, T. Takase, Y. Yoshida, H. Asanuma, *Angew. Chem. Int. Ed.* **2009**, *48*, 7044–7047.

[20] D. Baumstark, H.-A. Wagenknecht, *Angew. Chem. Int. Ed.* **2008**, *47*, 2612–2614.

[21] C. Wagner, H.-A. Wagenknecht, *Org. Lett.* **2006**, *8*, 4191–4194.

[22] T. A. Zeidan, R. Carmieli, R. F. Kelley, T. M. Wilson, F. D. Lewis, M. R. Wasielewski, *J. Am. Chem. Soc.* **2008**, *130*, 13945–13955.

[23] A. Mishra, R. K. Behera, P. K. Behera, B. K. Mishra, G. B. Behera, *Chem. Rev.* **2000**, *100*, 1973–2011.

[24] K. Hosoi, A. Hirano, T. Tani, *J. Appl. Phys.* **2001**, *90*, 6197–6204.

[25] a) E. Privat, U. Asseline, *Bioconjugate Chem.* **2001**, *12*, 757–769; b) R. Lartia, U. Asseline, *Chem. Eur. J.* **2006**, *12*, 2270–2281.

[26] a) X. Wang, U. J. Krull, *Bioorg. Med. Chem. Lett.* **2005**, *15*, 1725–1729; b) W. R. Algar, M. Massey, U. J. Krull, *J. Fluoresc.* **2006**, *16*, 555–567; c) U. Asseline, M. Chassignol, Y. Aubert, V. Roig, *Org. Biomol. Chem.* **2006**, *4*, 1949–1957.

[27] a) L. M. Wittenhagen, J. R. Carreon, E. G. Prestwich, S. O. Kelley, *Angew. Chem. Int. Ed.* **2005**, *44*, 2542–2546; b) K. P. Mahon Jr, M. D. Roy, J. R. Carreon, E. G. Prestwich, J. L. Rouge, S. Shin, S. O. Kelley, *ChemBioChem* **2006**, *7*, 766–773.

[28] J. R. Carreon, K. M. Stewart, K. P. Mahon, S. Shin, S. O. Kelley, *Bioorg. Med. Chem. Lett.* **2007**, *17*, 5182–5185.

[29] J. Brunner, J. K. Barton, *Biochemistry* **2006**, *45*, 12295–12302.

[30] N. Svanvik, J. Nygren, G. Westman, M. Kubista, *J. Am. Chem. Soc.* **2001**, *123*, 803–809.

[31] a) O. Seitz, F. Bergmann, D. Heindl, *Angew. Chem. Int. Ed.* **1999**, *38*, 2203–2206; b) D. V. Jarikote, O. Köhler, E. Socher, O. Seitz, *Eur. J. Org. Chem.* **2005**, 3187–3195; c) O. Köhler, O. Seitz, *Chem. Commun.* **2003**, 2938–2939; d) O. Köhler, D. V. Jarikote, O. Seitz, *Chem. Commun.* **2004**, 2674–2675.

[32] F. Menacher, M. Rubner, S. Berndl, H.-A. Wagenknecht, *J. Org. Chem.* **2008**, *73*, 4263–4266.

[33] S. Berndl, H.-A. Wagenknecht, *Angew. Chem. Int. Ed.* **2009**, *48*, 2418–2421.

[34] S. Laib, S. Seeger, *J. Fluoresc.* **2004**, *14*, 187–191.
[35] a) L. Zhang, A. E. Peritz, P. J. Carroll, E. Meggers, *Synthesis* **2006**, 645–653; b) M. K. Schlegel, L.-O. Essen, E. Meggers, *J. Am. Chem. Soc.* **2008**, *130*, 8158–8159.
[36] a) V. V. Filichev, U. B. Christensen, E. B. Pedersen, B. R. Babu, J. Wengel, *ChemBioChem* **2004**, *5*, 1673–1679; b) I. Geci, V. V. Filichev, E. B. Pedersen, *Chem. Eur. J.* **2007**, *13*, 6379–6386.
[37] P. M. E. Gierlich, S. Warncke, J. Gierlich, T. Carell, *Angew. Chem. Int. Ed.* **2008**, *47*, 3442–3444.
[38] D. I. Rozkiewicz, J. Gierlich, G. A. Burley, K. Gutsmiedl, T. Carell, B. J. Ravoo, D. N. Reinhoudt, *ChemBioChem* **2007**, *9*, 1997–2002.
[39] S. Berndl, N. Herzig, P. Kele, D. Lachmann, X. Li, O. Wolfbeis, H.-A. Wagenknecht, *Bioconjugate Chem.* **2009**, *20*, 558–564.
[40] a) R. Huber, N. Amann, H.-A. Wagenknecht, *J. Org. Chem.* **2004**, *69*, 744–751; b) N. Amann, R. Huber, H.-A. Wagenknecht, *Angew. Chem. Int. Ed.* **2004**, *43*, 1845–1847.
[41] a) C. Wanninger, H.-A. Wagenknecht, *Synlett* **2006**, 2051–2054; b) J. Barbaric, C. Wanninger-Weiß, H.-A. Wagenknecht, *Eur. J. Org. Chem.* **2009**, 364–370.
[42] C. Wagner, H.-A. Wagenknecht, *Org. Biomol. Chem.* **2008**, *6*, 48–50.
[43] N. Amann, H.-A. Wagenknecht, *Tetrahedron Lett.* **2003**, *44*, 1685–1690.
[44] a) E. B. Brauns, M. L. Madaras, R. S. Coleman, C. J. Murphy, M. A. Berg, *J. Am. Chem. Soc.* **1999**, *121*, 11644–11649; b) M. M. Somoza, D. Andreatta, C. J. Murphy, R. S. Coleman, M. A. Berg, *Nucleic Acids Res.* **2004**, *32*, 2494–2507.
[45] A. Trifonov, M. Raytchev, I. Buchvarov, M. Rist, J. Barbaric, H.-A. Wagenknecht, T. Fiebig, *J. Phys. Chem. B* **2005**, *109*, 19490–19495.
[46] S. Berndl, M. Breunig, A. Göpferich, H.-A. Wagenknecht, *Org. Biomol. Chem.*, manuscript submitted.
[47] H. S. Rye, S. Yue, D. E. Wemmer, M. A. Quesada, R. P. Haugland, R. A. Thies, A. N. Glazer, *Nucleic Acids Res.* **1992**, *20*, 2803–3812.
[48] a) S. Ikeda, T. Kubota, K. Kino, A. Okamoto, *Bioconjugate Chem.* **2008**, *19*, 1719–1725; b) S. Ikeda, T. Kubota, M. Yuki, A. Okamoto, *Angew. Chem. Int. Ed.* **2009**, *48*, 6480–6484.
[49] R. P. Haugland, *Handbook for Fluorescent Probes and Research Products*, 10th ed., Molecular Probes, Eugene, **2005**.

Received: December 7, 2009
Published Online: January 29, 2010

